

## Influence of The Substrate-Target Angle and Sputter Temperature On The Properties of CIGS Thin Films Sputtered From Single Quaternary Target

Filiz Keleş<sup>1,2,a,\*</sup>, Furkan Güçlüer<sup>2,3,b</sup>

<sup>1</sup> Department of Physics, Faculty of Arts and Sciences, Niğde Ömer Halisdemir University, Niğde, Türkiye.

<sup>2</sup> Nanotechnology Application and Research Center, Niğde Ömer Halisdemir University, Niğde, Türkiye.

<sup>3</sup> Department of Energy Science and Technologies, Niğde Ömer Halisdemir University, Niğde, Türkiye.

\*Corresponding author

### Research Article

#### History

Received: 31/01/2023

Accepted: 06/04/2023

#### Copyright



©2023 Faculty of Science,  
Sivas Cumhuriyet University

### ABSTRACT

In this study, Copper Indium Gallium Selenide (CIGS) thin films were successfully sputtered from a single quaternary target onto soda lime glass substrates. The effect of the incident angle of target atoms and sputter temperature on the properties of the films were examined using various techniques. It was found that a higher incident angle of target atoms resulted in a columnar microstructure, while a lower angle produced a solid film. The columnar structure showed improved optical absorption compared to the solid film. The sputter temperature had a greater effect on the crystalline properties of the films, with all films except those sputtered at room temperature showing polycrystalline formation. The films displayed a chalcopyrite structure and acceptable band gaps in the range of 1.1-1.3 eV, regardless of the incident angle and sputter temperature. These results indicate that the optical properties of CIGS thin films can be improved by a small increase in the incident angle of target atoms, without adversely affecting the structural and crystalline properties.

**Keywords:** CIGS thin film, RF magnetron sputtering, Oblique angle, Substrate temperature, Columnar structure.

<sup>a</sup> [fkeles@ohu.edu.tr](mailto:fkeles@ohu.edu.tr)

<sup>b</sup> <https://orcid.org/0000-0003-4548-489X>

[furkangucluer@hotmail.com](mailto:furkangucluer@hotmail.com)

<sup>b</sup> <https://orcid.org/0000-0002-8708-8994>

## Introduction

Chalcopyrite Cu(In,Ga)Se<sub>2</sub> (CIGS) is one of the most preferable absorber layers in thin-film solar cells with high efficiencies due to its tunable bandgap (1.04 – 1.68 eV) [1], high absorption coefficient ( $\sim 10^{15} \text{ cm}^{-1}$ ) [2] and high stability [3]. However, it is a challenging task to carry out a successful CIGS absorber layer deposition due to its quadruple component structure [4]. Three-stage co-evaporation process is the prominent method that is based on the simultaneous evaporation of multiple sources respectively at each stage [5, 6]. Although much progress has been made in fabrication of high-efficiency CIGS solar cell by this method [7], there are some drawbacks that limits its application in large scale devices. Since the evaporation of point sources of components (Cu, In, Ga, Se) is subjected, the CIGS film may not be uniformly coated. Besides, the difficulty of controlling the correct flux rates of the components usually results in the inhomogeneous elemental distribution through the CIGS. Another promising method for CIGS fabrication is the two-step process in which the metal precursors are sputtered followed by the post-selenization [8]. The Ga accumulation at the backside of CIGS thin film which is detrimental to the efficiency has usually been observed after the deposition of precursors. Therefore, the post-selenization process is offered as an inevitable solution [8, 9]. Although healing in the structural properties of CIGS could be achieved, the complexity and high-cost necessity

of the post-selenization are the side effects. Besides, the chemical used for selenium supplement during post-selenization is hazardous for human health.

A more practical and effective way of deposition of CIGS absorber layer is the single-step sputtering by using a quaternary target [10-14]. Sputtering directly from a single target provides good uniformity of thin film and simplification of process by eliminating the post-selenization-which paves the way for mass production along with the reduced material cost [15-18]. Nevertheless, further improvements in structural, morphological, and optical properties CIGS absorber layers deposited by single-step sputtering would be beneficial via additional practical attempts. It has attracted our attention that there is not any related study on how the incident angle of target species according to the substrate normal affects the film properties although there are many reports about some other parameters such as post-annealing [19] and bandgap engineering [20].

In this study, we introduce the way of varying the properties of CIGS thin film at two different incoming angles of elements that compose the Cu(In,Ga)Se<sub>2</sub> thin film. As the details will be given in the experimental section, the morphology and thus the related properties have differed when the angle has changed to 60° from the existing incident angle of 40°. Besides, the effect of the temperature has also been evaluated at these two

different angles. It was found that the incident angle of CIGS atoms is more effective on the morphology of the films while the structural and optical properties can be better properly controlled by the substrate temperature during the sputter.

## Materials and Methods

The deposition of CIGS thin films was performed by one-step RF magnetron sputtering (Nanovak NVTS-400). Soda-lime glass (SLG) substrates with 25 mm x 25 mm x 1mm dimensions were ultrasonically cleaned sequentially in acetone for 5 minutes, isopropanol for 5 minutes, and distilled (DI) water for 10 minutes, followed by drying with N<sub>2</sub> gas. The clean glass substrates were placed onto the holder and transferred into the deposition chamber. 2-inch diameter and 0.25-inch-thick single quaternary CuIn<sub>0.7</sub>Ga<sub>0.3</sub>Se<sub>2</sub> target with 99.99% purity was preferred for sputtering. Prior to the sputtering process, the base pressure of the chamber was pumped down below  $2 \times 10^{-6}$  Torr. The working gas pressure of high-purity Argon (Ar) was set to the 8 mTorr equivalent to the 4.3 sccm flow rate. The sputtering was carried out at the power of 95 W and the substrate rotation of 8 rpm to provide the homogenous film formation during all depositions.

In our study, we mainly focused on how the CIGS films are affected under two different incident angles of the incoming target atoms. The film composed on the substrate surface may have a dense or porous microstructure based on whether the target atoms reach to the substrate directly or obliquely. The dense film is obtained in case of the low incident angles of the impinging target atoms with respect to the substrate

normal because of the stacked layer-by-layer formation. On the other hand, the impinging atoms tend to form a porous film with columnar microstructure at highly oblique angles due to the cluster formation at the beginning of the deposition. When the angle of incidence is high, the incoming target atoms pile up and form randomly assembled islets on the film surface due to the phenomenon called the "shadowing effect" [21-23] which can be explained as the formerly clusters' shadowing the later atoms. These islets continue to grow and join each other during the sputtering process, and thus a porous, thin film that has a columnar type of microstructure is formed eventually. The approximate angle between target and substrate in our existing sputtering is 40° at which we can successfully deposit conventional thin films. We increased the angle to ~ 60° by simply raising the target holder little bit in the lateral position, as schematically described in Figure 1. Additionally, we investigated the effect of deposition temperature as well on the structural and optical properties of CIGS thin films grown at different angle configurations. As can be interpreted, the distance between the substrate and target would also change along with the varying angle. Therefore, we set the same thickness for all deposited films under various angles and temperatures in terms of performing a confident comparison. The same amount of deposited material because of setting the same thickness can be provided with the help of mass loading values using quartz crystal microbalance (QCM) [24]. The details of the CIGS thin films grown under different incident angles and temperatures are given in Table I.

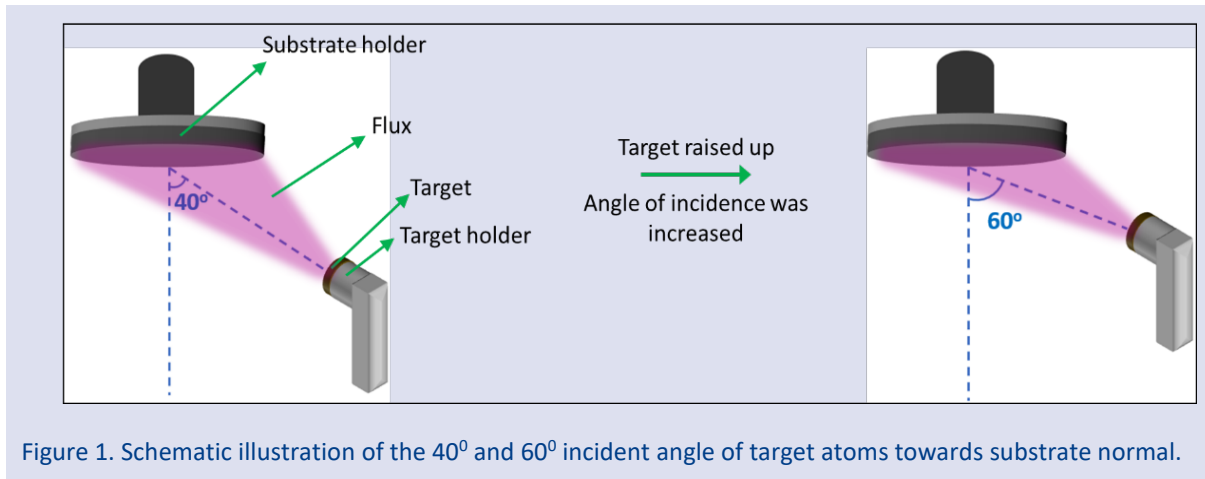


Figure 1. Schematic illustration of the 40° and 60° incident angle of target atoms towards substrate normal.

Table 1. The list of the CIGS thin films grown under various sputter parameters.

Sample Name	Deposition Temperature (°C)	Incident Angle (Degrees)
1	Room Temperature	40
2	150	40
3	300	40
4	Room Temperature	60
5	150	60
6	300	60

The morphological study of the CIGS thin films was conducted by Scanning Electron Microscope (SEM, FEI QUANTA FEG 250). The compositional properties were examined by Raman spectroscopy (Renishaw Raman-SPM/AFM) with the laser source at a wavelength of 633 nm. The crystallinity of the films was investigated by XRD Diffractometer (Malvern Panalitical Empyrean) with Cu-K $\alpha$  radiation ( $\lambda = 0.54$  nm). The absorption measurements were carried out by UV-Vis-NIR (Jasco V-670) Spectrophotometer at a wavelength range of 400-2500 nm.

## Results & Discussion

Cross-sectional SEM images of CIGS samples obtained under different incident angles of target atoms and deposition temperatures are shown in Figure 2. Columnar structure formation is apparent in thin films deposited at higher angle of 60° (Figure 1d-f) while relatively more planar and smooth thin films are formed in conventional configuration with an angle of 40° (Figure 2a-c). The main reason behind the difference in the microstructure

formation is the shadowing effect [22] that becomes significant when the arriving atoms reach the substrate at higher oblique angles. In our case, the shadowing effect which results in columnar formation is observed at the angle of 60° since the target atoms have a more oblique trajectory towards the substrate. The incident angle of target atoms not only affects the microstructure but also changes the thickness of the films. The thickness of the samples grown at 40° and 60° (room temperature) is approximately 1.1  $\mu\text{m}$  and 1.6  $\mu\text{m}$ , respectively, as shown in Figure 2a and Figure 2d in which the difference is the most significant among all films. The difference in thicknesses can be attributed to the microstructure of the films. Since the mass loading values were set the same, the film with columnar formation would be longer compared to conventional thin film because of the gaps between the columns. Despite the difference in the morphology from the side-view, the surface of the films seems almost the same as concluded from the top-view SEM images (not shown).

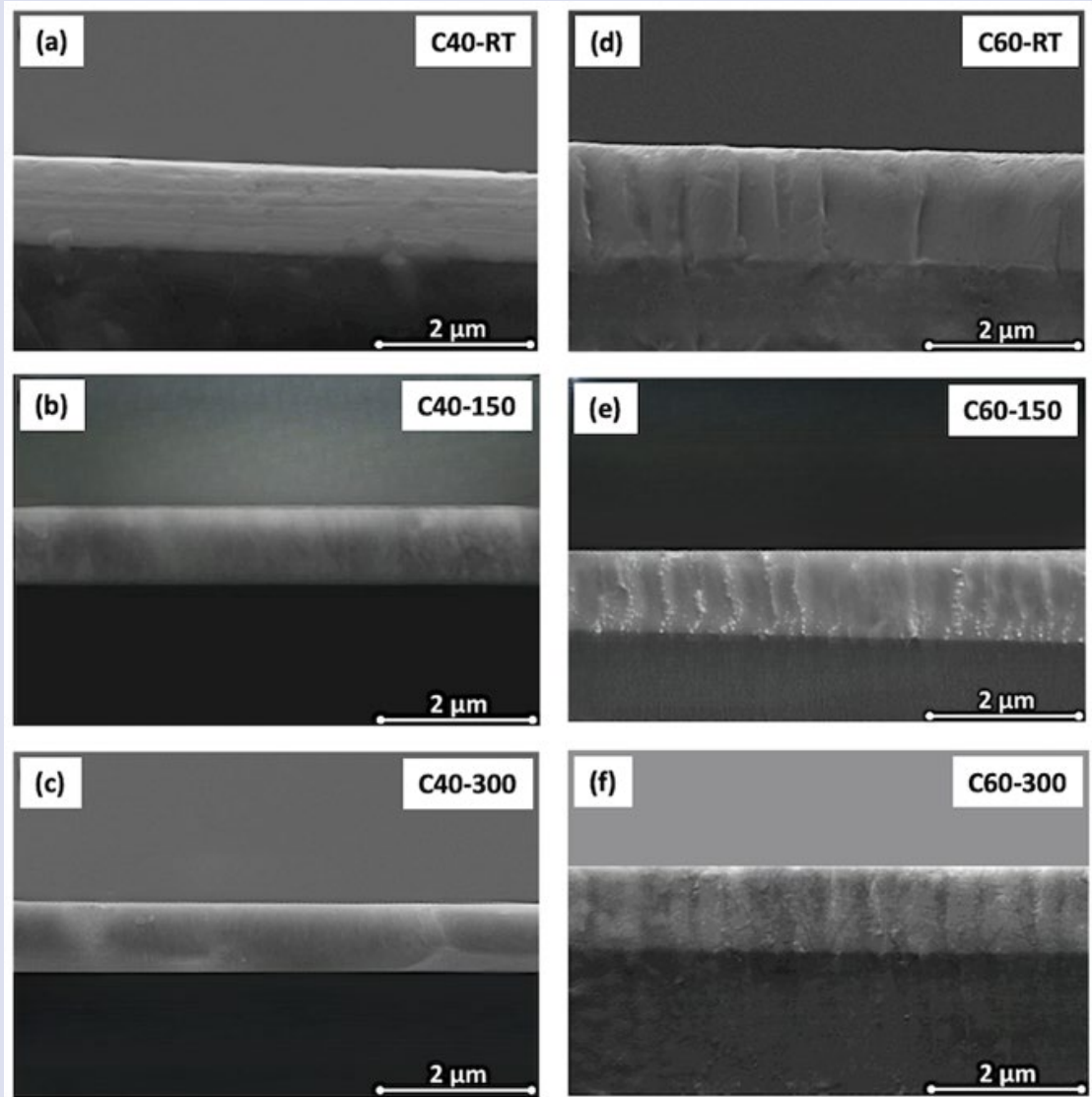


Figure 2. Cross-sectional SEM images of CIGS thin films grown under 40° of incident angle (a-c) and 60° of incident angle (d-f) at different substrate temperatures.

On the contrary, the temperature does not have a significant effect on the morphology of the films. The thickness of the films slightly decreases at temperatures

of 150°C and 300°C which is a well-known result from the literature [25].

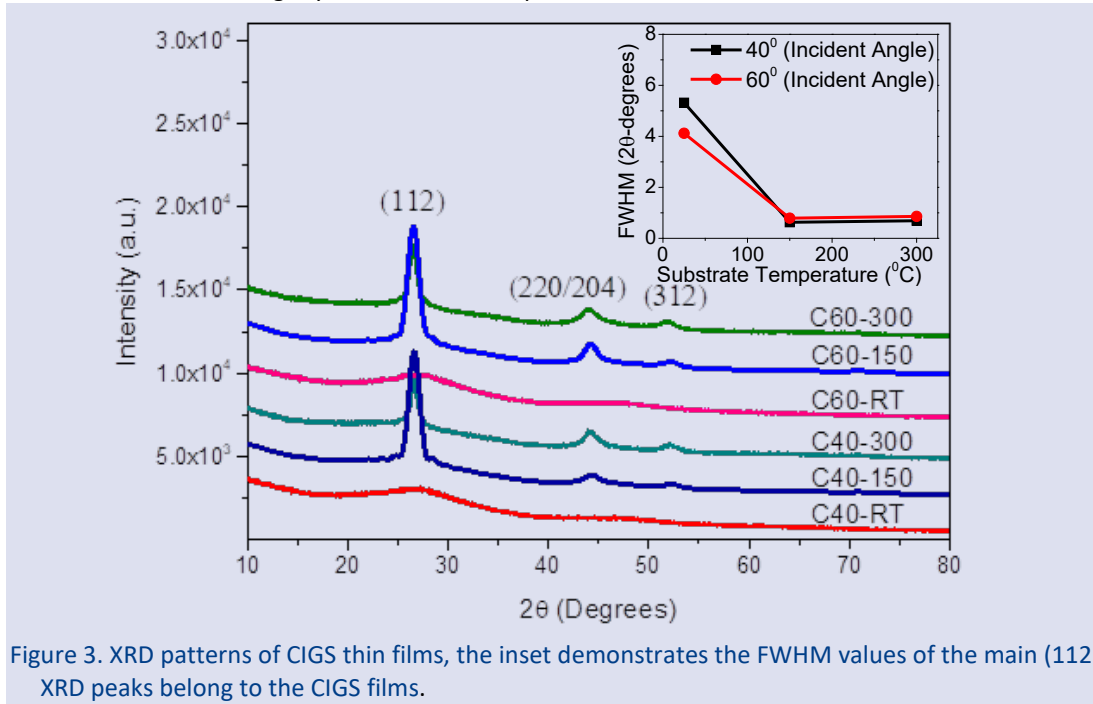
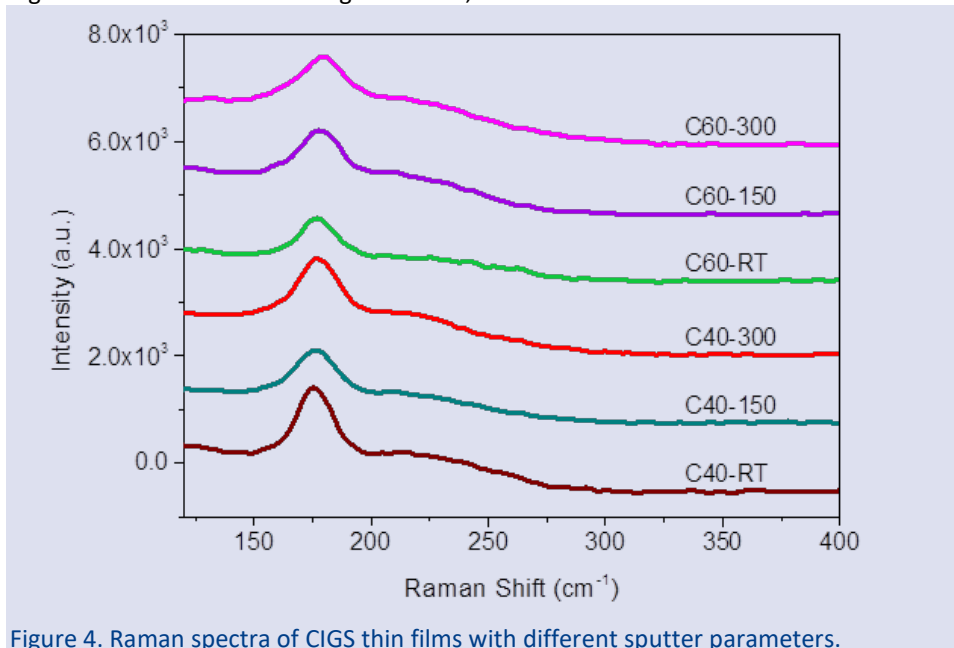


Figure 3 shows the XRD patterns of the samples deposited at different temperatures and the incident angle of target atoms. The most apparent fact concluded from the graph is that there is no obvious peak for the samples obtained at room temperature. While all the remaining films exhibit one strong and two weak peaks located at approximately 2-theta of 26, 44, and 52 degrees, which are correlated to the (112), (220/204), and (312) planes, respectively. It can be interpreted that the crystalline formation occurs only when the substrate temperature is applied during the sputtering process regardless of the incident angle. Indeed, the dramatic

decrement in FWHM of the main peak of the films obtained even at low temperature is demonstrated in the inset of Figure 3. On the other hand, both incident angles of 40° and 60° have no significant effect on the crystalline properties. The XRD data verifies the polycrystalline structure of CIGS thin films in the form of the chalcopyrite phase [12, 13, 26]. Thus, the fact that the kinetic energy of target atoms provided by the applied temperature is the main parameter that affects the crystalline formation while the incoming trajectory of the atoms towards the substrate alters the morphology of the films without having any impact on the crystallinity.



Raman spectra, a useful tool to investigate the chemical composition and phases of the films, are shown in Figure 4. All the films demonstrate a dominant peak located in the range of  $174\text{-}179\text{ cm}^{-1}$  that can be correlated to the  $A_1$  mode of the  $A_1B_{III}C_2V_1$  chalcopyrite compounds [27-30]. Since there is only  $A_1$  mode which is the most frequent and strong among all and no other obvious peak is observed in the spectra, it can be interpreted that all films obtained under different temperatures and substrate-target configurations exhibit the chalcopyrite formation. When it is recalled that the films grown at room temperature do not provide any prominent XRD peak while the  $A_1$  Raman mode is obtained from the same samples, it can be safely stated that the

films are in chalcopyrite phase with polycrystalline form regardless of the crystalline quality of the films. In addition, since no second phase peak is formed like  $Cu_2Se$  in the Raman spectrum curves, it can be said that a single-phase thin film structure was obtained [31]. FWHM values of  $A_1$  mode of the Raman curves was also examined. Although FWHM of the films obtained from main peak,  $174\text{-}179\text{ cm}^{-1}$ , do not differ significantly (in the range of  $17\text{-}21\text{ cm}^{-1}$ ), it was noticed that there is a slight broadening in FWHM of the samples for which temperature applied during growth. This finding may be attributed to the decay in phonon lifetime as a result of growth temperature [32].

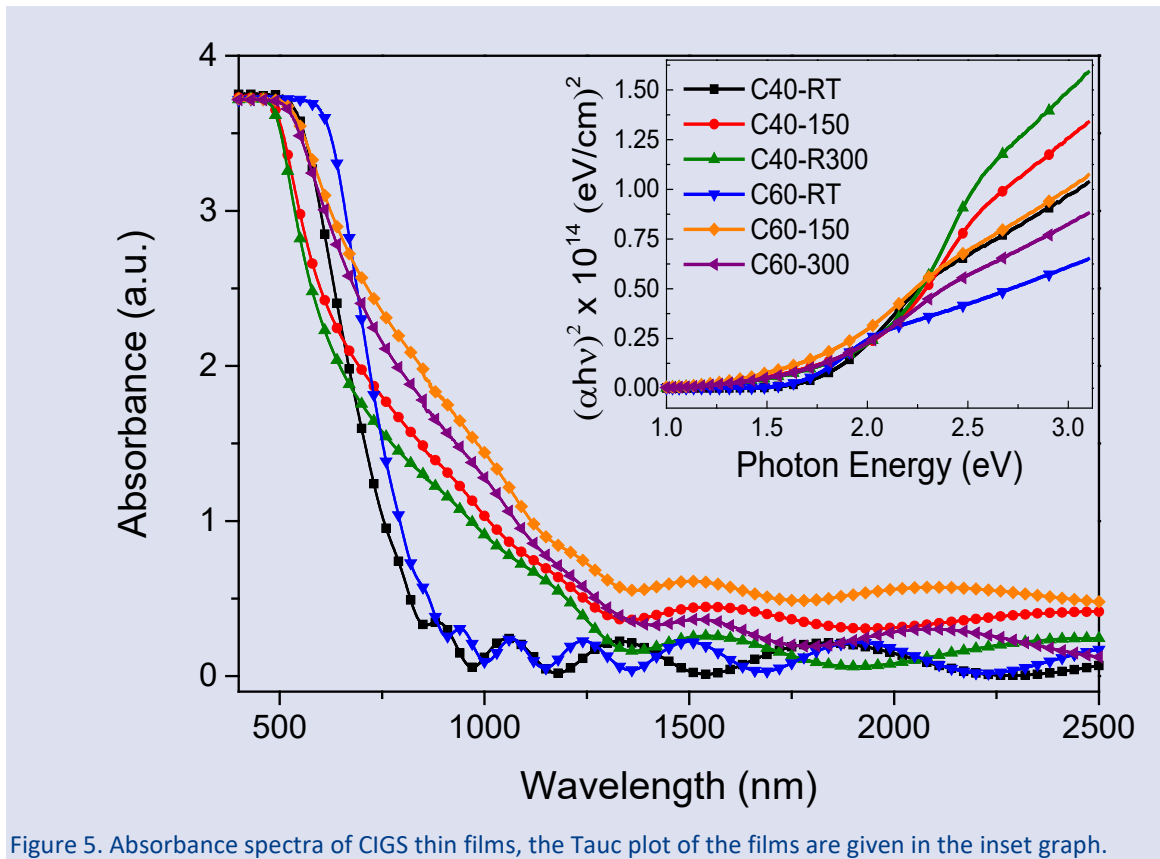


Figure 5. Absorbance spectra of CIGS thin films, the Tauc plot of the films are given in the inset graph.

The wavelength-dependent absorbance graph of the CIGS samples is demonstrated in Figure 5. The absorption enhancement in the near-infrared region ( $\sim 700\text{-}2500\text{ nm}$ ) for the samples grown with the temperature of  $150^\circ\text{C}$  and  $300^\circ\text{C}$  is the most remarkable observation at first glance. As compatible with the literature [33], the fact that crystallinity is improved even at low temperatures ( $150^\circ\text{C}$ ) could be expressed as the main reason for the higher absorption. On the other hand, the slight increment in absorption for each film deposited with a higher incident angle of  $60^\circ$  compared to its counterpart film obtained with a lower angle of  $40^\circ$  is another important observation that should be evaluated. The absorption enhancement for the samples obtained at higher incident angle of  $60^\circ$  can be attributed to the columnar microstructure of the films (Figure 2), which may be attributed to the slight

diminishing in bandgap. As the bandgap decreases, it is expected that there would be an increment in Urbach tail shown in absorbance spectra [34]. Since we only observe a slight increment in Urbach tail for the samples grown at higher angles, the above statement can be accepted for our case as making a true correlation between SEM images (Figure 2) and absorbance graph (Figure 5). Moreover, the ripple-like behavior at longer wavelength range for all samples regardless of temperature and incident angle is due to the thin film formation of the samples. The slightly higher thickness of the films grown at room temperature as shown in Figure 2 yields more ripples in longer wavelength range.

The optical bandgap of the films was estimated from Tauc's equation,  $(\alpha hv)^2 = A \cdot (hv - E_g)^{1/2}$  in the range of  $\sim 1.1\text{-}1.3\text{ eV}$  [34]. The inset in Figure 5 shows  $(\alpha hv)^2$  graphs versus the frequency-dependent energy ( $hv$ ),



where  $\alpha$  is the absorption coefficient,  $h$  is Planck's constant, and  $\nu$  is the frequency. The bandgap is extrapolated from the intersection of the line drawn through the linear part of the Tauc's plot with the x-axis (photon energy) [35]. Although there is not any significant trend in terms of the bandgap of the films, the bandgap increment by the temperature can be evaluated as the general interpretation from the inset graph. As the temperature increases, the thermal energy required for the deposited CIGS molecules to interact with each other is provided. Thus, more molecules interact, and the grain size is enhanced which results in the widening bandgap [37]. The slight enhancement in bandgap for the films sputtered under the incident angle of  $60^\circ$  compared to their counterparts can be attributed to the morphological and elemental differences which may result from their material densities [22].

## Conclusion

In summary, we have conducted the sputtering of CIGS thin films from a single quaternary target under two different incident angles of target atoms and various substrate temperatures. The most significant observation is that the incident angle of target atoms is more effective on the microstructure formation and absorption while substrate temperature plays an important role in crystallinity. Regardless of the temperature, the columnar-like and solid films are obtained at  $60^\circ$  and  $40^\circ$  degrees of incident angle, respectively. On the other hand, the crystalline formation concluded from XRD data only shows up when the temperature is applied during sputtering. Indeed, the films obtained under both incident angles demonstrate better crystallinity even at low temperature of  $150^\circ\text{C}$ . In addition, all films considered in this study have the chalcopyrite structure provided by Raman spectra. The slightly higher absorption of the films deposited with an angle of  $60^\circ$  compared to their counterparts is another significant conclusion. It was also observed that the bandgap values for all films obtained by Tauc's relation are close to each other and between 1.1-1.3 eV, although there is slight increment for the films when the temperature is applied during the growth. To sum up, we have revealed that the morphology and optical absorption of CIGS thin films can be improved by simply changing the substrate-target configuration while the chalcopyrite formation and crystallinity of the films are ensured even at low substrate temperature. In this regard, it can be predicted that the optical properties of high-quality CIGS thin films can be further improved by accordingly tuning the substrate-target configuration.

## Acknowledgements

The deposition and characterization of the CIGS thin films was carried out in Nanotechnology Application and Research Center at Nigde Ömer Halisdemir University. The authors would like to thank Selçuk University Physics Department for UV-Vis-NIR spectroscopy measurements.

## Conflicts of interest

There are no conflicts of interest in this work.

## References

- [1] Dullweber T., Rau U., Contreras M. A., Noufi R., Schock H. W., Photogeneration and carrier recombination in graded gap Cu (In, Ga) Se/sub 2/solar cells, *IEEE Trans. Electron Devices*. 47 (2000) 2249–2254.
- [2] Han S. H., Hermann A. M., Hasoon F. S., Al-Thani H. A., Levi D. H., Effect of Cu deficiency on the optical properties and electronic structure of CuInSe 2 and CuIn 0.8 Ga 0.2 Se 2 determined by spectroscopic ellipsometry, *Appl. Phys. Lett.* 85 (2004) 576–578.
- [3] Huang Y., Tang Y., Yuan W., Wang Q., Zhang S., Influence of surface-modified Mo back contact on post-selenized Cu (In, Ga) Se2 thin films, *Mater. Sci. Semicond. Process.* 57 (2017) 227–232.
- [4] Ramanujam J., Singh U. P., Copper indium gallium selenide based solar cells—a review, *Energy Environ. Sci.* 10 (2017) 1306–1319.
- [5] Yin L., Zhang K., Luo H., Cheng G., Ma X., Xiong Z., Xiao X., Highly efficient graphene-based Cu (In, Ga) Se 2 solar cells with large active area, *Nanoscale*. 6 (2014) 10879–10886.
- [6] Jung S., Ahn S. J., Yun J. H., Gwak J., Kim D., Yoon K., Effects of Ga contents on properties of CIGS thin films and solar cells fabricated by co-evaporation technique, *Curr. Appl. Phys.* 10 (2010) 990–996.
- [7] Jackson P., Hariskos D., Wuerz R., Kiowski O., Bauer A., Friedlmeier T. M., Powalla M., Properties of Cu (In, Ga) Se2 solar cells with new record efficiencies up to 21.7%, *Phys. Status Solidi (RRL)—Rapid Res. Lett.* 9 (2015) 28–31.
- [8] Huang P. C., Sung C. C., Chen J. H., Hsiao R. C., Hsu C. Y., Effect of selenization and sulfurization on the structure and performance of CIGS solar cell, *J. Mater. Sci. Mater. Electron.* 29 (2018) 1444–1450.
- [9] Liang H., Avachat U., Liu W., Van Duren J., Le M., CIGS formation by high temperature selenization of metal precursors in H2Se atmosphere, *Solid. State. Electron.* 76 (2012) 95–100.
- [10] Chen C. H., Lin T. Y., Hsu C. H., Wei S. Y., Lai C. H., Comprehensive characterization of Cu-rich Cu (In, Ga) Se2 absorbers prepared by one-step sputtering process, *Thin Solid Films*. 535 (2013) 122–126.
- [11] Ouyang L., Zhao M., Zhuang D., Han J., Gao Z., Guo L., Li X., Sun R., Cao M., Annealing treatment of Cu (In, Ga) Se2 absorbers prepared by sputtering a quaternary target for 13.5% conversion efficiency device, *Sol. Energy*. 118 (2015) 375–383.
- [12] Wang Q., Zhao Z., Li H., Zhuang J., Ma Z., Yang Y., Zhang L., Zhang Y., One-step RF magnetron sputtering method for preparing Cu (In, Ga) Se2 solar cells, *J. Mater. Sci. Mater. Electron.* 29 (2018) 11755–11762.
- [13] Yan Y., Li S., Ou Y., Ji Y., Yan C., Liu L., Yu Z., Zhao Y., Structure and properties of CIGS films based on one-stage RF-sputtering process at low substrate temperature, *J. Mod. Transp.* 22 (2014) 37–44.
- [14] Zhang L., Yu Y., Yu J., Wei Y., Effects of annealing atmosphere on the performance of Cu (InGa) Se2 films sputtered from quaternary targets, *R. Soc. Open Sci.* 7 (2020) 200662.
- [15] Chen C. H., Shih W. C., Chien C. Y., Hsu C. H., Wu Y. H., Lai C. H., A promising sputtering route for one-step fabrication of chalcopyrite phase Cu (In, Ga) Se2 absorbers without extra Se supply, *Sol. Energy Mater. Sol. Cells*. 103 (2012) 25–29.

- [16] Wang Y. H., Ho P. H., Huang W. C., Tu L. H., Chang H. F., Cai C. H., Lai C. H., Engineering a Ga-Gradient by One-Step Sputtering to Achieve Over 15% Efficiency of Cu (In, Ga) Se<sub>2</sub> Flexible Solar Cells without Post-selenization, *ACS Appl. Mater. Interfaces*. 12 (2020) 28320–28328.
- [17] Frantz J. A., Bekele R. Y., Nguyen V. Q., Sanghera J. S., Bruce A., Frolov S. V., Cyrus M., Aggarwal I. D., Cu (In, Ga) Se<sub>2</sub> thin films and devices sputtered from a single target without additional selenization, *Thin Solid Films*. 519 (2011) 7763–7765.
- [18] Lin T. Y., Lai C.H., Grading G., CIGS solar cell by one-step sputtering from a quaternary target without post-selenization, in: *2015 IEEE 42nd Photovolt. Spec. Conf., IEEE, 2015*: pp. 1–4.
- [19] Chen J., Shen H., Zhai Z., Li J., Wang W., Shang H., Li Y., Effect of substrate temperature and post-annealing on the properties of CIGS thin films deposited using e-beam evaporation, *J. Phys. D: Appl. Phys.* 49 (2016) 495601.
- [20] Yan L., Bai Y., Yang B., Chen N., Tan Z., Hayat T., Alsaedi A., Extending absorption of near-infrared wavelength range for high efficiency CIGS solar cell via adjusting energy band, *Curr. Appl. Phys.* 18 (2018) 484–490.
- [21] Keles F., Cansizoglu H., Badraddin E. O., Brozak M. P., Watanabe F., Karabacak T., HIPS-GLAD core shell nanorod array photodetectors with enhanced photocurrent and reduced dark current, *Mater. Res. Express*. 3 (2016) 105028.
- [22] Keles F., Badrdeen E., Karabacak T., Self-anti-reflective density-modulated thin films by HIPS technique, *Nanotechnology*. 28 (2017) 335703.
- [23] Badrdeen E., Brozak M, Keles F., Al-Mayalee K., Karabacak T., High performance flexible copper indium gallium selenide core-shell nanorod array photodetectors, *J. Vac. Sci. Technol. A Vacuum, Surfaces, Film*. 35 (2017) 03E112.
- [24] Nakano T., Baba S., Gas pressure effects on thickness uniformity and circumvented deposition during sputter deposition process, *Vacuum*. 80 (2006) 647–649.
- [25] Liu G. S., Li H. N., Shen X. Y., Hu Z. Q., Hao H. S., Effect of Substrate Temperature on One-Step Magnetron-Sputtered Cu (In, Ga) Se<sub>2</sub> Thin Films for Solar Cells, in: *Appl. Mech. Mater., Trans Tech Publ, 2013*: pp. 703–707.
- [26] Zhang H. X., Hong R. J., CIGS absorbing layers prepared by RF magnetron sputtering from a single quaternary target, *Ceram. Int*. 42 (2016) 14543–14547.
- [27] Witte W., Kniese R., Powalla M., Raman investigations of Cu (In, Ga) Se<sub>2</sub> thin films with various copper contents, *Thin Solid Films*. 517 (2008) 867–869.
- [28] Roy S., Guha P., Kundu S. N., Hanzawa H., Chaudhuri S., Pal A. K., Characterization of Cu (In, Ga) Se<sub>2</sub> films by Raman scattering, *Mater. Chem. Phys.* 73 (2002) 24–30.
- [29] Huang X., Miao X., Yu N., Guan X., Effects of deposition profiles on RF-sputtered Cu (In, Ga)Se<sub>2</sub> films at low substrate temperature, *Appl. Surf. Sci.* 287 (2013) 257–262.
- [30] Shi J. H., Li Z. Q., Zhang D. W., Liu Q. Q., Sun Z., Huang S. M., Fabrication of Cu (In, Ga) Se<sub>2</sub> thin films by sputtering from a single quaternary chalcogenide target, *Prog. Photovoltaics Res. Appl.* 19 (2011) 160–164.
- [31] Nagaoka A., Nose Y., Miyake H., Scarpulla M. A., Yoshino K., (2015). Solution growth of chalcopyrite compounds single crystal. *Renewable Energy*, 79, 127-130.
- [32] Ruiz C. M., Fontané X., Fairbrother A., Izquierdo-Roca V., Broussillou C., Bodnar Bermudez V. (2012, June). Developing Raman scattering as quality control technique: Correlation with presence of electronic defects in CIGS-based devices. In 2012 38th IEEE Photovoltaic Specialists Conference (pp. 000455-000458). IEEE.
- [33] Yu Z., Yan Y., Li S., Zhang Y., Yan C., Liu L., Zhang Y., Zhao Y., Significant effect of substrate temperature on the phase structure, optical and electrical properties of RF sputtered CIGS films, *Appl. Surf. Sci.* 264 (2013) 197–201.
- [34] Dhanaraj A., Das K., Keller J. M., A Study of The Optical Band Gap Energy and Urbach Energy of Fullerene (C60) Doped PMMA Nanocomposites, *AIP Conference Proceedings*. 2270 (2020) 110040.
- [35] Mankoshi M. A. K., Mustafa F. I., Hintaw N. J., Effects of Annealing Temperature on Structural and Optical Properties of CIGS Thin Films for Using in Solar Cell Applications, in: *J. Phys. Conf. Ser., IOP Publishing, 2018*: p. 12019.
- [36] Chandramohan M., Velumani S., Venkatachalam T., Experimental and theoretical investigations of structural and optical properties of CIGS thin films, *Mater. Sci. Eng. B*. 174 (2010) 205–208.
- [37] Wang H., Zhang Y., Kou X. L., Cai Y. A., Liu W., Yu T., Pang J. B., Li C. J., Sun Y., Effect of substrate temperature on the structural and electrical properties of CIGS films based on the one-stage co-evaporation process, *Semicond. Sci. Technol.* 25 (2010) 55007.